Measles as a Case Study in Nonlinear Forecasting and Chaos

B. T. Grenfell, A. Kleczkowski, S. P. Ellner and B. M. Bolker

Email alerting service   Receive free email alerts when new articles cite this article - sign up in the box at the top right-hand corner of the article or click **here**

Measles as a case study in nonlinear forecasting and chaos†

By B. T. Grenfell[1], A. Kleczkowski[2], S. P. Ellner[3] and B. M. Bolker[4]

[1] *Zoology Department, Cambridge University, Downing Street, Cambridge CB2 3EJ, U.K.*
[2] *Department of Plant Sciences, Cambridge University, Downing Street, Cambridge CB2 3EA, U.K.*
[3] *Statistics Department, North Carolina State University, Raleigh, North Carolina, U.S.A.*
[4] *Department of Ecology and Evolutionary Biology, Princeton University, Princeton, New Jersey 08544-1003, U.S.A.*

This paper uses measles incidence in developed countries as the basis of a case study in nonlinear forecasting and chaos. It uses a combination of epidemiological modelling and nonlinear forecasting to explore a range of issues relating to the predictability of measles before and after the advent of mass vaccination. A comparison of the pre-vaccination self-predictability of measles in England and Wales indicates relatively high predictability of these predominantly biennial epidemic series, compared to New York City, which shows mixtures of one-, two- and three-year epidemics. This analysis also indicates the importance of choosing correct embeddings to avoid bias in prediction. Forecasting for English cities indicates significant spatial heterogeneity in predictability before vaccination and an overall drop in predictability during the vaccination era. The interpretation of predictions of observed measles series by epidemiological models is explored and areas for refinement of current models discussed.

---

1. Introduction

The pattern of measles epidemics in developed countries is one of the best documented population cycles in ecology. The availability of long disease notification series and the comparatively simple natural history of infection have prompted an extensive empirical and theoretical literature on the population biology of the infection. This work has concentrated on two main areas. First, the public health importance of measles (still a major killer in developing countries (Mclean & Anderson 1988)) has generated a large and distinguished body of quantitative epidemiological research, focusing in particular on the origin and perpetuation of epidemics, the persistence of measles as a function of community size and the impact on vaccination strategies of various heterogeneities in transmission (Hamer

---

† This paper was produced from the authors' disk by using the TEX typesetting system.

© 1994 The Royal Society

1906; Soper 1929; Bartlett 1957, 1960; Dietz & Schenzle 1985; May 1986; London & Yorke 1973; Anderson & May 1982, 1985, 1991; Dietz 1976). Second, the last decade has considerable interest in the pattern of measles incidence as a potential ecological candidate for deterministic chaos (Schaffer & Kot 1985; Olsen *et al.* 1988; Olsen & Schaffer 1990; Kot *et al.* 1988; Schaffer 1985a; Rand & Wilson 1991; Sugihara & May 1990). It is still an open question as to whether measles dynamics are chaotic but, in any case, the debate and in particular the work of W. M. Schaffer and his co-workers (Schaffer & Kot 1985; Olsen *et al.* 1988; Olsen & Schaffer 1990; Kot *et al.* 1988; Schaffer 1985a), has been highly stimulating to population ecologists and epidemiologists alike.

Recently, Tidd *et al.* (1993), building on the work of Sugihara & May (1990), have used nonlinear prediction to examine evidence for chaos in measles. They analysed observed pre-vaccination time series from a number of cities and towns in developed countries, comparing the self-predictability of these series with forecasts generated by a range of empirical and mechanistic epidemiological models. From this analysis, they proposed evidence for chaos, reflected by a decline in internal predictability of the observed series with the time step of prediction. They also found that the mechanistic epidemiological models out-performed empirical statistical formulations in predicting the observed series.

Tidd *et al.*'s paper raises a number of issues about nonlinear forecasting, which we examine in this paper.

(1) *How does the detailed pattern of pre-vaccination epidemics affect the prediction process?*

The main contrast here is between a predominantly biennial sequence of major epidemics (typified by the pattern in English cities during the 1950s and 60s; figure 1*b–i* and time series such as that for New York City (figure 1*a*), which show occasional epidemics with a period of three years (Grenfell *et al.* 1993; Bolker & Grenfell 1993; Olsen *et al.* 1988). Tidd *et al.* (1993) concentrate on the latter case, focusing mainly on developed country cities, such as New York, which contain three-year epidemics. Here, we assess the predictive implications of these different patterns, based on a comparative analysis of series from England and Wales and New York City.

(2) *How does mass vaccination affect patterns of predictability?*

Mass vaccination against measles began in the 1960s and is now applied (to a greater or lesser extent) throughout the world. Assessing the predictability of measles epidemics in the face of vaccination is obviously the most important applied forecasting issue. In this paper, we therefore examine the impact of vaccination on the nonlinear predicability of measles epidemics in England and Wales.

(3) *How do epidemiological models perform in predicting observed measles series?*

As reviewed in detail below, the comparatively simple natural history of measles infection has led to considerable success in the construction of epidemiological models. These range from the simple homogeneous SEIR model to models incorporating age, spatial structure and other heterogeneities (Bartlett 1957, 1960; Black 1966; Hamer 1906; Soper 1929; Schenzle 1984; Anderson & May 1991). Tidd *et al.* (1993) found that epidemiological models perform better as predictors of observed measles series than empirical linear models. Such comparisons
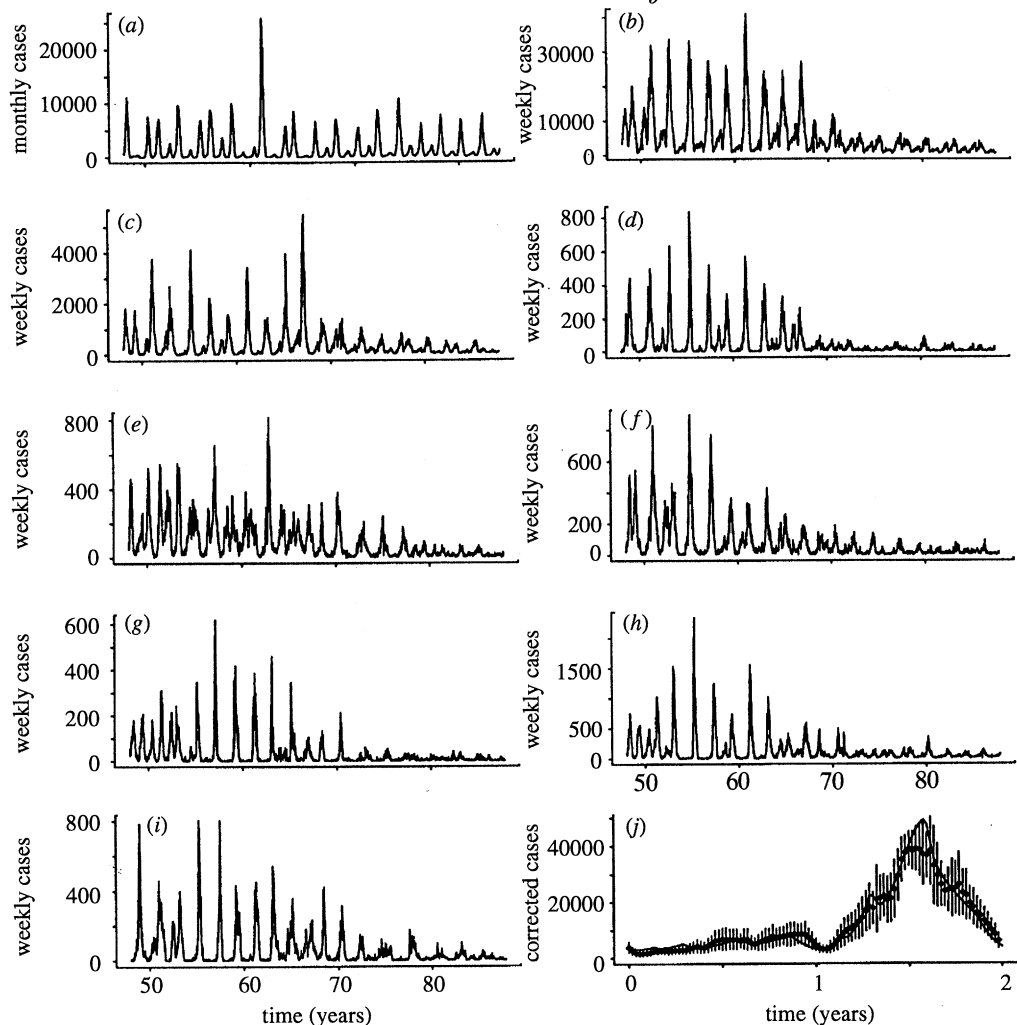
Figure 1. (*a*)–(*i*) Time series of measles notifications in New York City, England and Wales and seven English cities. The monthly New York data were kindly provided by L.F. Olsen and the weekly UK data are from the Weekly Returns of the Office of Population Censuses and Surveys. (*j*) Comparison of the observed biennial pattern of cases in England and Wales, scaled up by a factor 1.4 to allow for notification efficiency (Bolker & Grenfell 1992) with the best fit of the RAS model as described in the text (see Bolker & Grenfell (1992) for full details). The observed mean pattern is shows as a dotted line (bars represent ±1 standard deviation) and the model dynamics (a stable biennial limit cycle) as a solid line.(*a*) New York, pre-vaccination; (*b*) England and Wales, (*c*) London, (*d*) Bristol, (*e*) Liverpool, (*f*) Manchester, (*g*) Newcastle, (*h*) Birmingham, (*i*) Sheffield, (*j*) RAS model for E+W.

are valuable, however, as discussed below, there are various statistical and epidemiological complexities which affect their interpretation.

The following section defines the data-sets and prediction algorithm used. We then briefly review current knowledge about measles dynamics, based on an assessment of how the available models perform in reflecting observed patterns. This serves as a conceptual basis for subsequent sections, which address the questions set out above.

2. Data sources and statistical methods

(a) The data

The analysis centres on notification time series for New York City in the era before vaccination and for seven English cities (and the England and Wales aggregate) before and after the advent of vaccination. These data are displayed and documented in figure 1. Measles vaccination in England and Wales began in earnest in 1968 (Fine & Clarkson 1982a) and caused a significant reduction in average disease incidence, with a relative stabilization of average cases from 1972 until the mid 1980s (figure 1b–i). We therefore take the pre- and post-vaccination series from the periods 1948–67 and 1972–86 respectively. To facilitate comparison with the (monthly) New York data, as well as to avoid possibilities of oversampling (Sugihara *et al.* 1990), the weekly England and Wales series shown in figure 1 are summed into four weekly periods before analysis.

(b) Estimating nonlinear predictability

Extensive reviews of nonlinear forecasting techniques are given by Tong (1990) and Yao & Tong (this volume). For purposes of comparison, we use the same algorithm as Tidd *et al.* (1993). This is a simple zero order ϵ-ball method (Tong 1990; Farmer & Sidorowich 1987), with slight modifications, as described below.

(*a*) To assess the self-predictability of an observed time series, scaled on (0,1), separate the data into two halves; the first half (the atlas) is used to predict the second (the target series). To predict observed series from simulated model series, scale the observed and model series independently on (0,1) (Tidd *et al.* 1993), then take the simulated series as the atlas and the full observed series as the target.

(*b*) Embed the data in a delayed coordinate space (embedding dimension E and delay, d time units).

(*c*) For each point in the embedded target series, select all atlas points within a radius ϵ of the observed point. By default, ϵ is set at 0.1 in scaled coordinates and this common radius for all target points is expanded so that at least one atlas point is within the ϵ-ball. Following Tidd *et al.* (1993), we restrict the maximum number of points in the atlas to 10.

(*d*) For each lead time step, the target and atlas points are projected forwards one step and the mean of the latter is used as the prediction. If the maximum lead time is T, the last T points in the target (and the initial atlas) are omitted, so that all predictions are based on the same number of atlas points and the same number of predictions are done for each prediction time step. The relative success of prediction is assessed by an R^2 between observed and predicted points; the regression slope between observed and predicted series is calculated to assess bias in the predictions.

Sugihara *et al.* (1990) used differenced data to assess predictability in English cities. Here, we follow Tidd *et al.* (1993), analysing the raw notification data, for comparison with their results.

3. Modelling measles dynamics

(a) The SEIR model

The simplest description of measles infection dynamics is the well known SEIR (susceptible–exposed–infectious–recovered) model, which has a long history of study in mathematical epidemiology (Hamer 1906; Soper 1929; Kermack & McKendrick 1927, 1932, 1933; May 1986; Anderson & May 1991; Dietz & Schenzle 1985). It is expressed as a set of three nonlinear ordinary differential equations:

$$\frac{dS}{dt} = \mu N(1-p) - (\mu + \beta I)S, \quad \frac{dE}{dt} = \beta I S - (\mu + \sigma)E, \quad \frac{dI}{dt} = \sigma E - (\mu + \gamma)I. \tag{3.1}$$

S, E, I and R respectively represent the density of susceptible, exposed, infectious and recovered individuals, in a constant total population of size $N = S + E + I + R$. Average per capita mortality rate due to all causes is μ years^{-1}; given that infection is assumed not to cause extra mortality, the net birth (μN) and death ($\mu[S + E + I + R]$) rates are equal. In this simplest version of the model (which ignores maternally derived immunity in infants), individuals are assumed to be born susceptible, with vaccination effectively at birth moving a proportion p of susceptibles into the recovered class.

During natural measles infection, susceptible individuals are assumed to move through the exposed and infectious classes, at rates σ and γ years^{-1} respectively, and then become immune to reinfection, entering the recovered class for life. The net infection rate, IS, is controlled by the infection parameter β years^{-1} infective^{-1}.

Seasonality. There is a significant annual variation in measles incidence, mainly associated with changes in the contact rate of children caused by the seasonal pattern of school terms (Fine & Clarkson 1982b; London & Yorke 1973). Several workers have modelled the effects of seasonal variations in infection rate (London & Yorke 1973; Dietz 1976; Grossman 1980; Aron & Schwartz 1984; Aron 1990; Schaffer & Kot 1985; Schenzle 1984). The simplest approach is to replace the constant infection parameter, β, of equations (3.1) with a time-varying periodic function, such as

$$\beta(t) = b_0[1 + b_1 \cos(2\pi t)], \tag{3.2}$$

Here, b_0 is the average infection rate and b_1 controls the amplitude of variation around it.

(b) Modelling the impact of age-structure: the RAS model

The infection parameter, $\beta(t)$, of the seasonally forced SEIR model is assumed to be independent of age, spatial structure or other heterogeneities. Along with spatial structure, heterogeneities in infection rate with age – and specifically the concentration of infection in school children – have been shown to be of considerable importance, both to measles dynamics and the projected impact of vaccination strategies (Dietz & Schenzle 1985; Fine & Clarkson 1982b; Anderson & May 1991). These age-specific heterogeneities in transmission are also intimately bound up with the seasonal variations in infection rates noted above (Fine & Clarkson 1982b). This interaction has been modelled by Schenzle (1984), who developed a continuous time age-cohort formulation which mimics the average pre-vaccination pattern of measles epidemics in England and Wales very closely

(figure 1*j*), as well as the qualitative behaviour of the infection after the onset of vaccination. We now briefly review the dynamics of this relatively complex formulation (which is called the realistic age-structured (RAS) model below), compared to those of the standard SEIR model.

(i) *Deterministic dynamics*

SEIR model   For high degrees of seasonal forcing ($b_1 > 0.28$), the SEIR model exhibits large-amplitude chaos (Aron & Schwartz 1984; Schaffer 1985*b*; Schaffer & Kot 1985; Olsen & Schaffer 1990; Rand & Wilson 1991). Recent work also indicates the possibility of complex dynamics at lower degrees of forcing, particularly under the influence of process noise (Rand & Wilson 1991) and spatial heterogeneity (Engbert & Drepper 1994). Although a strongly forced SEIR model can generate patterns of one-, two- and three-year cycles which are qualitatively similar to real measles time series (Olsen & Schaffer 1990), the troughs between major three-year epidemics are generally much too deep to be realistic (Bolker & Grenfell 1993; Grenfell 1992). Although this problem is alleviated somewhat by allowing for immigration of infectives (Engbert & Drepper 1993), there are still more potential fadeouts of infection (i.e. periods with incidence below one infective) than observed.

RAS model   The deterministic dynamics of the more biologically complex RAS model are dynamically simpler than those of the SEIR (Bolker & Grenfell 1993). The RAS model characteristically generates limit cycles (figure 1*j*), without the unrealistically deep troughs of the SEIR model.

(ii) *Stochastic dynamics*

Given the propensity of seasonally forced measles models for deep troughs in incidence, it is important to explore the impact of demographic stochasticity on their dynamics. Figure 2 compares the dynamics of stochastic realizations of the seasonally forced SEIR model and the RAS model, assuming a total population size of $N = 1$ million. These simulations use a standard Monte Carlo framework (first applied to measles in the seminal work of Bartlett (1957, 1960); full details are given by Bolker & Grenfell (1993). Model parameters are chosen so that the corresponding deterministic dynamics generate chaotic (SEIR) and stable biennial (RAS) patterns of epidemics. The SEIR model generates a time series (figure 2*a*) reflecting irregular mixtures of one-, two- and three-year cycles. The large amplitude three-year cycles generate frequent extinctions of infection, which are not observed in practice in cities (Bartlett 1960) or islands (Black 1966) of population size 1 million.

By contrast to the major difference in their deterministic dynamics, the stochastic RAS and SEIR time series show qualitatively similar patterns (Bolker & Grenfell 1993). In particular, the RAS model time series (figure 2*b*) exhibits mixtures of one-, two- and three-year cycles broadly similar to the SEIR results, again with unrealistically large numbers of fadeouts of infection. For reasons that are not yet clear, significant demographic noise destabilises the limit cycle behaviour of the deterministic RAS model.

In summary, the deterministic RAS model provides a good fit to observed biennial measles epidemics in England and Wales. However, versions of the RAS and SEIR models which encorporate demographic stochasticity cannot capture the observed persistence of measles in urban communities (Bolker & Grenfell 1993).
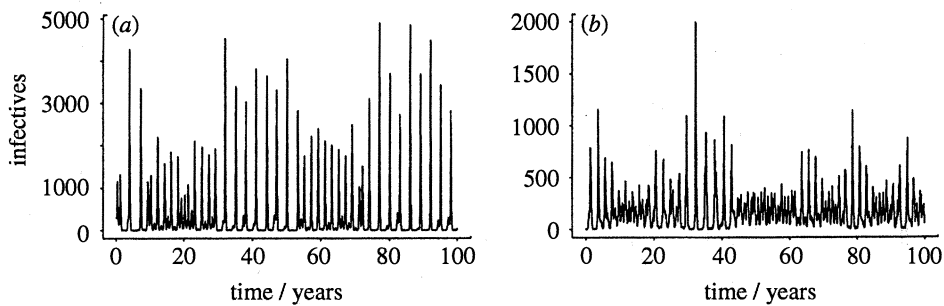
Figure 2. Monte Carlo simulations of the SEIR and RAS models, assuming a total population size of $N = 1$ million. Simulations, by standard Monte Carlo methods (Grenfell 1992) were run for 200 years before recording results. The SEIR simulation uses the parameter set: $\mu = 0.02$ years^{-1}, $p = 0$, $b_0 = 0.0010107$ years^{-1}infective^{-1}, $b_1 = 0.28$, $\sigma = 48.67$ years^{-1}, $\gamma = 56.19$ years^{-1}, it and the RAS simulation are described fully by Bolker & Grenfell (1992). Infection is restarted after fadeout by a Poisson 'immigration' of infectives, with mean 21 years^{-1}. (*a*), (*b*) Time series of infectives generated by SEIR and RAS models respectively. Although the SEIR and RAS simulations show diferent mean levels of infection (reflecting slightly different epidemiological assumptions (Bolker & Grenfell 1993)), they exhibit the same qualitative pattern: a mixture of one-, two- and three-year epidemic cycles.

Though including explicit spatial structure into the RAS model alleviates this problem somewhat (Bolker 1994), further refinements to the models are clearly needed, as discussed below.

4. Results

These are grouped according to the questions raised in §1.

(*a*) *Patterns of self-predictability in measles data*

(i) *England and Wales before vaccination*

Figure 3*a* shows the prediction profile (the pattern of prediction R^2 against prediction time) for the pre-vaccination measles incidence time series for the whole of England and Wales. We explore various embedding dimensions and lags, focusing first on the embedding used by Tidd *et al.* (1993) for their New York City analysis: embedding dimension $E = 4$ and lag $d = 1$ month. The basic pattern that Tidd *et al.* derive for New York and other cities is a more or less monotonic decline in predictability with prediction time. By contrast, our results for England and Wales (the solid line in figure 3*a*) show a sharp decline in predictability, from $R^2 \approx 0.8$ at a 1 month prediction time step to $R^2 \approx 0.2$ and 6 months, followed by a steady rise back to 80% by 24 months and then a decline.

This pattern for $E = 4$, lag $d = 1$ is explored further in figure 3*b, c*. Figure 3*b* plots observed against predicted points (open circles) for a prediction time of 6 months (corresponding to the minimum predictability in figure 3*a*). The slope of this relationship is effectively zero over most of the range of the observations indicating a severe downward bias in the predictions. In order to understand this bias, we show a detailed analysis of the prediction process for one target point, along with the equivalent predicted trajectory and the projections of individual atlas points which are averaged to produce it. This picture (figure 3*c*) makes the source of the bias very clear. The embedding used is unable to separate adjacent points in the time series, so that the atlas consists of lagged copies
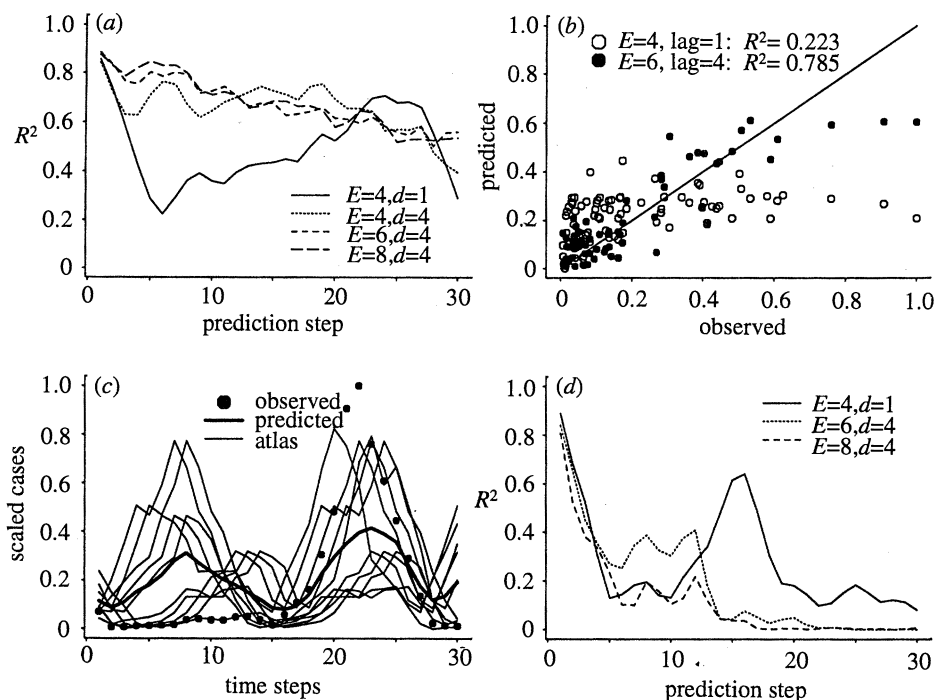
Figure 3. Basic prediction results for the pre-vaccination England and Wales time series of four-weekly measles case reports. Details of the plots are given in the text. (a) Prediction profiles at various embeddings; (b) observed against predicted points for the 6 month prediction step (the observed=predicted line is also displayed), with two different embeddings as shown; (c) detailed analysis of the prediction for a typical target point; (d) prediction profiles for the New York City data for various embeddings.

of a small number of epidemics. The resulting predicted trajectory shows an annual pattern, which quickly diverges from the observations as the prediction time increases from one month. Though the predicted pattern does somewhat better in representing the observations at 24 months, this is an artifact of the annual periodicity in the data. As reflected in figure 3b, the predictions therefore also consistently underestimate major epidemics.

Returning to figure 3a, this problem is alleviated if either embedding dimension or embedding lag are increased. In particular, if embedding lag is increased to 4 months, the prediction profile is much flatter, and shows only a slow decline over a 24 month prediction time. Figure 3b includes a typical plot of observed against expected points for $E = 6$, $d = 4$ (solid dots), the slope is now not significantly different from unity over most of the range of the observations, indicating that this greater degree of embedding is required to remove the bias. Figure 3b also indicates that there is a downward bias in the predictions for very high observed points. This is simply because the largest epidemic peaks are in the second (target) half of the series.

(ii) *New York City before vaccination (figure 3d)*

For predictions up to 12 months ahead, the prediction profile for $E = 4$, $d = 1$ is very similar to the declining pattern of R^2 reported by Tidd *et al.* (1993).
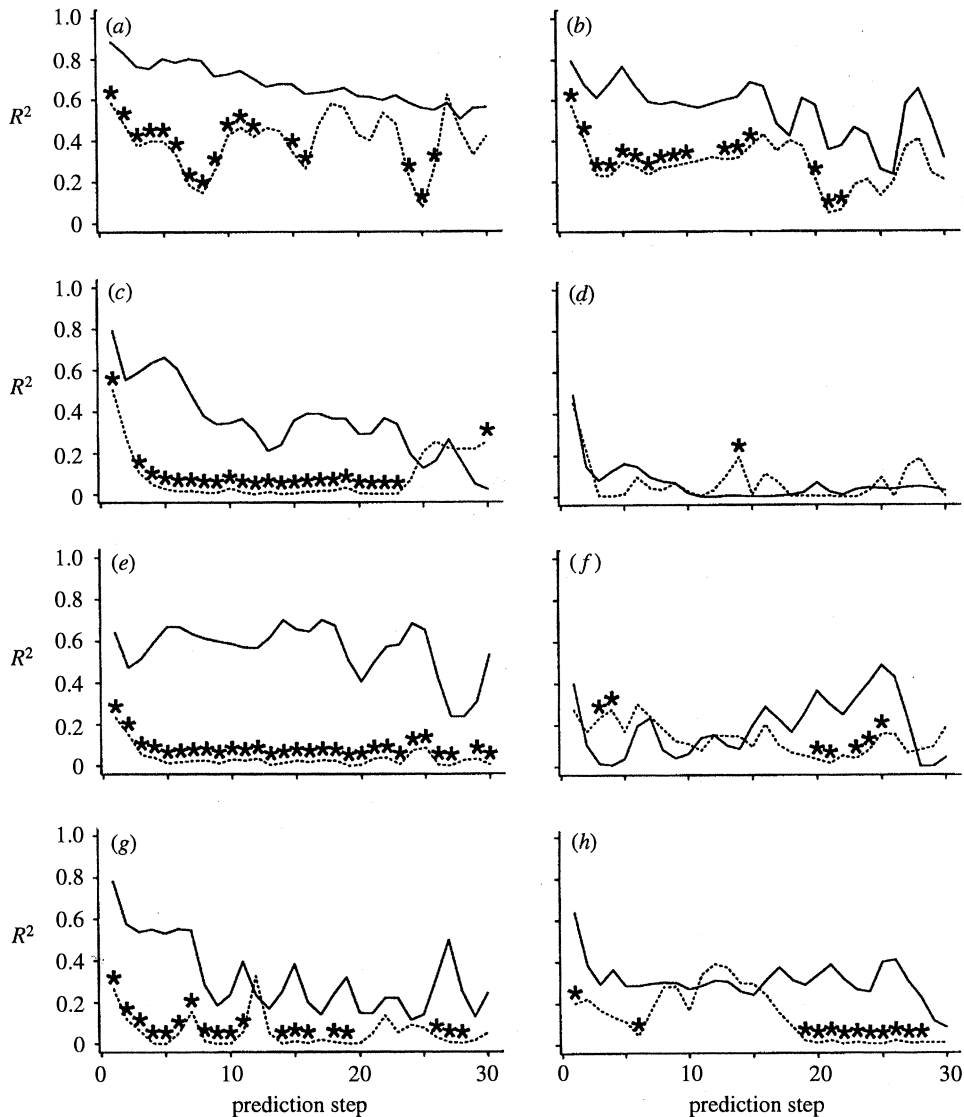
Figure 4. Prediction profiles ($E = 6$, $d = 4$) for the pre-vaccination (solid line) and vaccination eras (dotted line) for England and Wales and English cities. Stars indicate significant ($p < 0.05$) differences between pre-vaccination and vaccination correlation coefficients, based on a standard Fisher's z transformation. (*a*) England and Wales, (*b*) London, (*c*) Bristol, (*d*) Liverpool, (*e*) Manchester, (*f*) Newcastle, (*g*) Birmingham, (*h*) Sheffield.

However, if as shown in figure 3*d*, we extend the analysis beyond 12 months, we discover a sharp peak in prediction R^2 at around 15 months. Figure 4, also shows results for higher embedding dimensions and lags; in essence, these reduce the peak at 15 months, producing a much more consistent decline in R^2.

We do not explore these patterns further here, though they do underline the general point that the detailed structure of the observed series has a strong influence on patterns of predictability (Yao & Tong, this volume). For example,

the first half of the New York City time series (figure 1*a*) shows a mixture of annual epidemics and a large three-year epidemic, while the second half is essentially biennial. It may therefore be that the second half is relatively predictable (as is the regular biennial pattern of England and Wales), but not from an atlas constructed from the first half. Choice of which part of the series forms the atlas is clearly crucial here (Sugihara *et al.* 1990). In any case, these results further illustrate the marked differences between the pre-vaccination England and Wales and New York series (Grenfell *et al.* 1994).

(iii) *The impact of vaccination*

Figure 4 shows prediction profiles for England and Wales and seven English cities, before and after the onset of vaccination. To minimize the biases discussed above, the analysis is based on the embedding $E = 6$, $d = 4$. Two general points emerge from this analysis. First, the predictability of the post-vaccination series is, in general significantly lower than that before vaccination. Further analysis (not shown here) indicates that this difference is not due to the shorter time series used in the vaccination era. Instead, it arises mainly from the greater irregularity in measles incidence after the onset of vaccination. This is apparent in the time series in figure 1 – vaccination reduces the major, predictable epidemics seen before the vaccine era (Anderson *et al.* 1984; Dietz & Schenzle 1985; Anderson & May 1991). Time series analysis (Bolker & Grenfell 1994) also indicates that the spatial coherency of epidemics is lower after the onset of vaccination than in the pre-vaccine era.

Second (and surprisingly), there is no strong trend for average pre-vaccination predictability to decrease with population size. Though a relatively small city, such as Newcastle (1960 population 290 000), is less predictable than London, the series for Manchester (700 000) and Birmingham (1 090 000) have more or less equivalent predictability. In fact differences in predictability are strongly influenced by the detailed structure of individual series. For example, although Manchester (figure 4*c*) and Liverpool (figure 4*d*) are of similar size and 20 miles apart, Liverpool is much less predictable in the pre-vaccination period. This happens because the pre-vaccination Liverpool time series (figure 1*e*) shows a preponderance of annual cycles in the first (atlas) half, which is not able to capture the more recent biennial cycles. Over the period considered, Liverpool has a significantly higher birth rate than the other major cities (Grenfell 1992), and (as will be discussed elsewhere) this probably causes its distinct measles dynamics. Interestingly, the predictability profiles for London (figure 4*b*) are similar to those for England and Wales as a whole (figure 4*a*), both before and after the onset of vaccination.

(b) *Forecasting measles incidence with epidemiological models*

We begin by considering the general strategy of assessing the forecasting ability of models, and then examine the performance of the RAS model in predicting the prevalence of the England and Wales series.

(i) *Assessing the fit of deterministic models*

Tidd *et al.* (1993) found that mechanistic models, such as the SEIR and RAS models, outperform a variety of stochastic empirical formulations based on surrogate data in predicting observed measles incidence. They adduced this as evidence
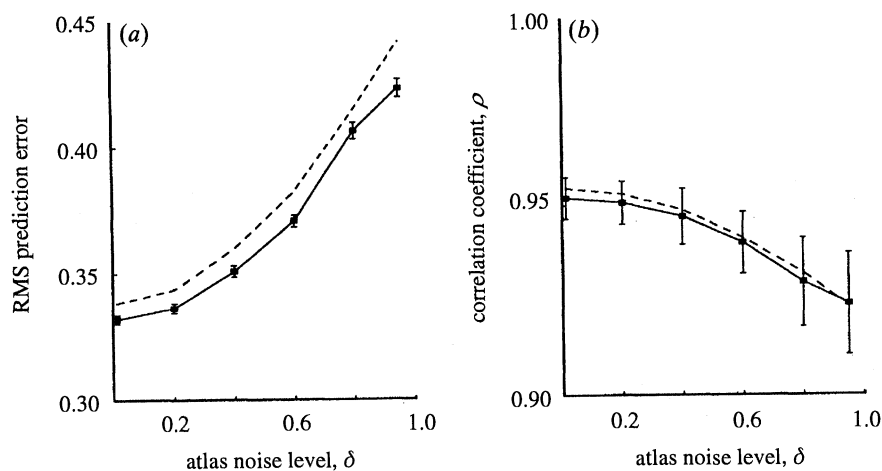
Figure 5. (a) Prediction error, and (b) correlation between 1-step ahead predicted and actual values in the ϵ-ball method of Tidd *et al.* (1993). The true dynamics are the Ricker model (equation (4.3) in the text) with $r = 3.25$ and noise level $\delta = 0.4$; the atlases were generated by the same model except that the noise level was varied between $\delta = 0$ and $\delta = 0.95$. For each data point, the prediction is based on its eight nearest neighbours in the atlas. The solid line in each panel shows the mean $+-$ one standard error over 100 replicate data/atlas pairs, using data series of length 250 and atlas series of length 500; the dashed line shows the expected value in the limit of an infinitely large atlas.

that deterministic models are better able to predict historic measles epidemics that their phenomenological counterparts. However, we believe that this conclusions is questionable, because their method is biassed in favour of deterministic models, even when the data come from a stochastic system. Suppose that (as in the models used by Tidd *et al.*) the true dynamics of the system can be written in the form,

$$X(t + 1) = F(X(t), \omega e(t + 1)), \tag{4.1}$$

where X is the state vector, F is a nonlinear map, ω is the noise level and $e(t)$ is a series of independent, identically distributed random variables ('noise'), with $e(t + 1)$ independent of $X(s)$ for $s = t, t - 1, \ldots$. (Correlated noise complicates our argument but the conclusion is the same.) Consider now how $X(t+1)$ can be predicted from observed values of $X(t), X(t-1), \ldots$. The optimal predictor in the sense of mean square error is the conditional mean $E(X(t+1)|X(t), X(t-1), \ldots)$, which for (4.1) is given by

$$E_{e(t)}\{FX(t), \omega e(t))\} \tag{4.2}$$

(Karlin & Taylor 1975, ch. 9). Note that expression (4.2) is always a deterministic function of past values of X, whether equation (4.1) is stochastic ($\omega > 0$) or deterministic ($\omega = 0$): the least-squares optimal predictor is a deterministic function of the information currently available. The same applies for prediction any number of steps into the future, and for continuous time dynamics. Figure 5 shows a specific example, using the procedures of Tidd *et al.* The true dynamics are a one-dimensional population model (the Ricker equation) perturbed by noise,

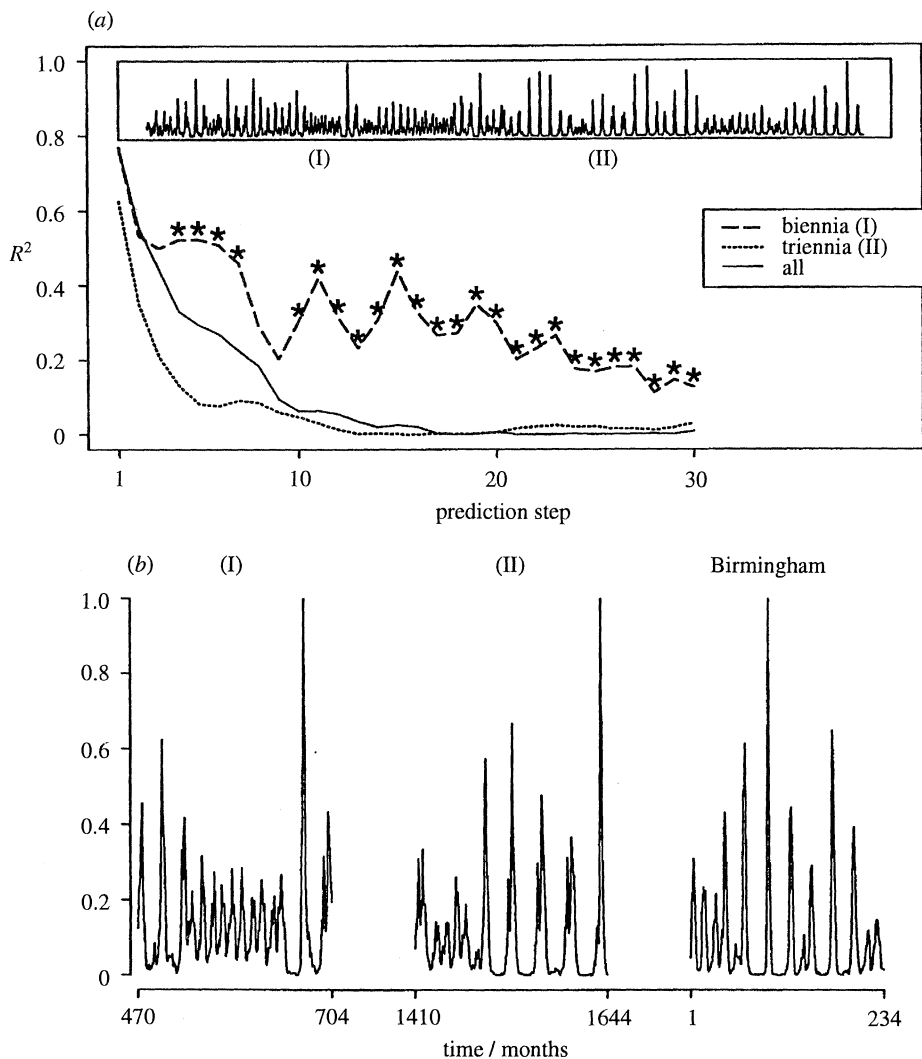$$x(t + 1) = x(t) \exp(r(1 - x(t))(1 + \omega e(t + 1)), \tag{4.3}$$

Figure 6. Predicting the pre-vaccination Birmingham measles time series with the stochastic version of the RAS model (see Bolker & Grenfell (1992) for full details). (a) Prediction profiles using the whole 100-year atlas (shown as an inset) and the two subsets (marked as (I) and (II) on the inset) described in the text. (b) Scaled (on (0,1)) versions of the two RAS subsets, compared with the observed Birmingham series. The stars in (a) indicate signficiant differences ($p < 0.05$) between correlation coefficients for the Birmingham fit based on atlas (II), compared with that for the total atlas.

where $e(t)$ is uniformly distributed on the interval $[-1, 1]$. For the true dynamics, the noise amplitude was $\delta = 0.4$. We varied the value of δ in the models used to construct the atlas for prediction with the ϵ-ball method of Tidd *et al.* (1993). In line with the arguments above, the optimal prediction atlas is achieved by the model with $\delta = 0$, not by the model with the true value of δ.

This phenomenon confounds Tidd *et al.*'s method of comparing alternative choices for the prediction model F in equation (4.1). Their procedure is to construct atlases using a variety of candidate models F_i. Each candidate F_i is at

best an approximation to the true F, so its prediction accuracy (using the correct value of ω) would be higher than that using the true dynamics (equation (4.1)). Thus, using a smaller-than-true ω would improve F_i's prediction accuracy, and make it closer to that of the true model. Tidd *et al.* constructed their atlas for epidemiological models using Monte Carlo realizations with relatively low noise levels, whereas for all of the alternative models the atlas was constructed with a higher degree of noise. They then interpreted the results as favouring the deterministic model. However, the comparison is biased by the intrinsic advantage of a deterministic model in their method. To avoid this bias, the comparison could be based instead on a conditional mean (expression (4.2)), which can be computed by simulation if it is not available in closed form.

(ii) *Model predictions for England and Wales*

Following Tidd *et al.* (1993), we use a Monte Carlo realization of an epidemiological model to forecast observed measles dynamics in a city of size 1 million. Birmingham is chosen as the closest city to this population size in the currently available data-set. Figure 6 gives details of various fits of the RAS model to the pre-vaccination Birmingham series. We concentrate on the RAS model here – preliminary studies with the SEIR model indicate qualitatively similar results to those reported below.

The basic forecast (figure 6) uses an atlas of 100 years of monthly Monte Carlo RAS output (shown in figure 6a) to predict the full pre-vaccination Birmingham series. The atlas and target series are scaled *independently* on (0,1) before embedding (Tidd *et al.* 1993). The resulting predictions show an essentially monotonic exponential decline in predictability with prediction time – this is qualitatively similar to the result for Copenhagen derived by Tidd *et al.* (1993). However, a detailed examination of the model series indicates a more complex picture. As described above, the RAS Monte Carlo simulation generates a mixture of large amplitude three-year cycles interspersed with periods of biennial and annual cycles. Scaling the whole series on (0,1), therefore reduces the effective amplitude of the biennial periods, so that they are not 'found' by the forecasting algorithm, leading to low apparent predictability beyond very short prediction times.

Figure 6b explores this further, by restricting the atlas to an 18-year period of predominantly biennial cycles in the RAS simulation, which visually resembles the observed series (period (II) in the figure). Scaling this period on (0,1) and forecasting from it produces a significant improvement in predictability, compared with predicting from the full atlas (figure 6a). Finally, choosing an 18-year atlas with triennial cycles (figure 6b, period (I)) produces a similar decline in predictability to the whole RAS atlas (figure 6a). Clearly, the choice of scaling has a major effect on the performance of the atlas in systems with intermittency.

5. Discussion

This paper has set out to show that the use of nonlinear prediction in epidemiology raises several complex issues, which we have covered relatively thinly in the space available. We therefore conclude by suggesting directions for future work.

528   *B. T. Grenfell, A. Kleczkowski, S. P. Ellner and B. M. Bolker*

(a) General forecasting issues

The central point to emerge here is the potential complexity of trying to forecast nonlinear systems which can exhibit more than one sort of behaviour. The situation is especially acute if (as may be the case with measles), the relatively short length of observed series (20–40 years) corresponds roughly to the timescale of qualitative changes in behaviour implied by the models. Our preliminary results with a simple prediction scheme depends critically on the detailed structure of the observed series. Not surprisingly, regular biennial patterns (such as in England and Wales) are relatively predictable, compared to more irregular patterns, including three-year cycles, observed for example in New York. More work is needed here to refine the comparisons using better algorithms, different choices of atlas to combat non-stationarity (Sugihara *et al.* 1990), data transformation and scaling and comparisons with parametric statistical models. The scaling problem is especially acute when using atlases from models. For example, using atlas and target series on absolute scales might be preferable to scaling on (0,1), but this still depends on the algorithm being sufficiently sensitive to choose the appropriate region of attractor behaviour. Sorting these problems out is essential before we can compare the predictive ability of models such as SEIR and RAS (Tidd *et al.* 1993).

(b) Epidemiological issues

(i) Modelling

Predictions based on models are difficult to interpret, unless we are confident that model behaviour is a correct mirror of real dynamics. For example, no observed measles series to our knowledge shows the periods of regular repeated three-year cycles generated by the stochastic SEIR and RAS models. This problem points to a need to refine existing measles models. As noted above, there is still much to understand about the spatial dynamics and persistence of measles, though other areas also need to be addressed. In particular, any attempt to predict the future from the past is likely to be fraught with danger if we do not take account of long term changes in underlying driving variables of the system. For childhood diseases such as measles, long term trends in birth rate (the 'engine' which ultimately drives measles epidemics) are likely to play a significant role in this context (Grenfell & Anderson 1985; Grenfell *et al.* 1994). Differences in birth rate in developed and developing countries have a marked effect on measles dynamics (Mclean & Anderson 1988; Grenfell *et al.* 1994), however, the effects of secular changes in birth rate have been much less studied.

Recently, Grenfell *et al.* (1994) have demonstrated associations between the post World War II 'baby boom' in birth rate and subsequent average measles incidence in English cities and Copenhagen. The increase in average measles incidence is reflected in the raw England and Wales data (figure 1) by a transition from annual dynamics in the late 1950s to biennial epidemics (Grenfell *et al.* 1994), and the length of this transition varies between cities. Teasing out whether this effect is due only to the intrinsic infection dynamics or is influenced by birth rates or other variables is important, both to the process of prediction and to interpreting any message about nonlinearity that prediction gives us. Analyses, based on more explicit models of family demography (Anderson & May 1991;

Phil. Trans. R. Soc. Lond. A (1994)

Becker 1989) are required to clarify the dynamic effects of demographic changes on measles incidence.

(ii) *Predictability and vaccination*

Finally, on an applied note, the important forecasting issue to clarify is the predictability of measles under the impact of vaccination, rather than in the pre-vaccination era (Tidd *et al.* 1993). Our preliminary results (based on the short and rather non-stationary series for England and Wales) indicate that predictability falls with vaccination, though this happens less in large centres such as London. More work is needed here, both to clarify the statistical issues and to decide whether achievable levels of forecastability are of any practical use, particularly given changes in vaccine uptake.

References

Anderson, R. M., Grenfell, B. T. & May, R. M. 1984 Oscillatory fluctuations in the incidence of infectious disease and the impact of vaccination: time series analysis. *J. Hyg. (Camb.)* **93**, 587–608.

Anderson, R. M. & May, R. M. 1982 Directly transmitted infectious diseases: control by vaccination. *Science, Wash.* **215**, 1053–1060.

Anderson, R. M. & May, R. M. 1985 Age-related changes in the rate of disease transmission: implications for the design of vaccination programmes. *J. Hyg. (Camb.)* **94**, 365–436.

Anderson, R. M. & May, R. M. 1991 *Infectious diseases of humans: dynamics and control.* Oxford University Press.

Aron, J. L. 1990 Multiple attractors in the response to a vaccination program. *Theor. Popul. Biol.* **38**, 58–67.

Aron, J. L. & Schwartz, I. B. 1984 Seasonality and period-doubling bifurcations in an epidemic model. *J. Theor. Biol.* **110**, 665–679.

Bartlett, M. S. 1957 Measles periodicity and community size. *Jl R. statist. Soc.* A **120**, 48–70.

Bartlett, M. S. 1960 The critical community size for measles in the U.S. *Jl R. statist. Soc.* A **123**, 37–44.

Becker, N. G. 1989 *Analysis of infectious disease data.* London: Chapman and Hall.

Black, F. L. 1966 Measles endemicity in insular populations: critical community size and its evolutionary implication. *J. Theor. Biol.* **11**, 207–211.

Bolker, B. M. & Grenfell, B. T. 1993 Chaos and biological complexity in measles dynamics. *Proc. R. Soc. Lond.* B **251**, 75–81.

Dietz, K. 1976 The incidence of infectious diseases under the influence of seasonal fluctuations. *Lect. Notes. Biomath.* **11**, 1–15.

Dietz, K. & Schenzle, D. 1985 Mathematical models for infectious disease statistics. In *A celebration of Statistics* (ed. A. C. Atkinson & S. E. Feinberg), pp. 167–204. New York: Springer.

Engbert, R. & Drepper, F. R. 1994 Qualitative analysis of unpredictability: a case study from childhood epidemics. In *Proc. Predictability and Nonlinear Modelling in Natural Sciences and Economics, 4–7 April 1993, Wageningen (NL).* (In the press.)

Farmer, J. D & Sidorowich, J. J. 1987 Predicting chaotic time series. *Phys. Rev. Lett.* **59**, 845–848.

Fine, P. E. M. & Clarkson, J. A. 1982a Measles in England and Wales. II. The impact of the measles vaccination programme on the distribution of immunity in the population. *Int. J. Epidem.* **11**, 15–25.

Fine, P. E. M. & Clarkson, J. A. 1982*b* Measles in England and Wales. I. an analysis of factors underlying seasonal patterns. *Int. J. Epidem.* **11**, 5–15.

Grenfell, B. T. 1992 Chance and chaos in measles dynamics. *Jl R. statist. Soc.* B **54**, 383–398.

Grenfell, B. T. & Anderson, R. M. 1985 The estimation of age-related rates of infection from case notifications and serological data. *J. Hyg. (Camb.)* **95**, 419–436.

Grenfell, B. T., Bolker, B. M. & Kleczkowski, A. 1994 Seasonality, demography, and the dynamics of measles in developed countries. In *Epidemic models: their structure and relation to data* (ed. D. Mollison). Cambridge University Press.

Grossman, Z. 1980 Oscillatory phenomena in a model of infectious diseases. *Theor. Popul. Biol.* **18**, 204–243.

Hamer, W. H. 1906 Epidemic disease in England – the evidence of variability and of persistency of type. *Lancet* **1**, 733–739.

Kermack, W. O. & McKendrick, A. G. 1927 A contribution to the mathematical theory of epidemics. *Proc. R. Soc. Lond.* A **115**, 700–721.

Kermack, W. O. & McKendrick, A. G. 1932 A contribution to the mathematical theory of epidemics. II. The problem of endemicity. *Proc. R. Soc. Lond.* A **138**, 55–83.

Kermack, W. O. & McKendrick, A. G. 1933 A contribution to the mathematical theory of epidemics. III. Further studies of the problem of endemicity. *Proc. R. Soc. Lond.* A **141**, 92–122.

Kot, M., Graser, D. J., Truty, G. L., Schaffer, W. M. & Olsen, L. F. 1988 Changing criteria for imposing order. *Ecol. Modelling* **43**, 75–110.

London, W. P. & Yorke, J. A. 1973 Recurrent outbreaks of measles, chickenpox and mumps. I. Seasonal variation in contact rates. *Am. J. Epidem.* **98**, 453–468.

May, R. M. 1986 Population biology of microparasitic infections. In *Biomathematics* (ed. T. G. Hallam & S. A. Levin), vol. 17, pp. 405–442. Berlin: Springer-Verlag.

Mclean, A. R. & Anderson, R. M. 1988 Measles in developing countries. I. Epidemiological parameters and patterns. *Epidemiol. Infect.* **100**, 111–133.

Olsen, L. F., Truty, G. L. & Schaffer, W. M. 1988 Oscillations and chaos in epidemics: a nonlinear dynamic study of six childhood diseases in Copenhagen, Denmark. *Theor. Popul. Biol.* **33**, 344–370.

Olsen, L. F. & Schaffer, W. M. 1990 Chaos versus noisy periodicity: alternative hypotheses for childhood epidemics. *Science, Wash.* **249**, 499–504.

Rand, D. A. & Wilson, H. 1991 Chaotic stochasticity: a ubiquitous source of unpredictability in epidemics. *Proc. R. Soc. Lond.* B **246**, 179–184.

Schaffer, W. M. 1985*a* Order and chaos in ecological systems. *Ecology* **66**, 93–106.

Schaffer, W. M. 1985*b* Can nonlinear dynamics elucidate mechanisms in ecology and epidemiology? *IMA J. Math. appl. Med. Biol.* **2**, 221–252.

Schaffer, W. M. & Kot, M. 1985 Nearly one dimensional dynamics in an epidemic. *J. Theor. Biol.* **112**, 403–427.

Schenzle, D. 1984 An age-structured model of pre- and post-vaccination measles transmission. *IMA J. Math. appl. Med. Biol.* **1**, 169–191.

Soper, M. A. 1929 The interpretation of periodicity in disease prevalence. *Jl R. statist. Soc.* A **92**, 34–61.

Sugihara, G., Grenfell, B. & May, R. M. 1990 Distinguishing error from chaos in ecological time series. *Phil. Trans. R. Soc. Lond.* B **330**, 235–251.

Sugihara, G. & May, R. M. 1990 Nonlinear forecasting as a way of distinguishing chaos from measurement error in time series. *Nature, Lond.* **344**, 734–741.

Tidd, C. W., Olsen, L. F. & Schaffer, W. M. 1993 The case for chaos in childhood epidemics. II. Predicting historical epidemics from mathematical models. *Proc. R. Soc. Lond.* B **254**, 257–273.

Tong, H. 1990 *Nonlinear time series: a dynamical systems approach.* Oxford University Press.